Diabetes-Induced DUSP4 Reduction Promotes Podocyte Dysfunction and Progression of Diabetic Nephropathy

Benoit Denhez,[1] Marina Rousseau,[1] David-Alexandre Dancosst,[1] Farah Lizotte,[1] Andréanne Guay,[1] Mannix Auger-Messier,[1,2] Anne Marie Côté,[1,3] and Pedro Geraldes[1,4]

Diabetes 2019;68:1026–1039 | https://doi.org/10.2337/db18-0837

Diabetic nephropathy (DN) remains the leading cause of end-stage renal disease. Hyperglycemia-induced podocyte dysfunction is a major contributor of renal function impairment in DN. Previous studies showed that activation of mitogen-activated protein kinase (MAPK) in diabetes promotes podocyte dysfunction and cell death. Dual specificity phosphatases (DUSPs) are a family of phosphatases mainly responsible for MAPK inhibition. In this study, we demonstrated that diabetes and high glucose exposure decreased DUSP4 expression in cultured podocytes and glomeruli. Diabetes-induced DUSP4 reduction enhanced p38 and c-Jun N-terminal kinase (JNK) activity and podocyte dysfunction. The overexpression of DUSP4 prevented the activation of p38, JNK, caspase 3/7 activity, and NADPH oxidase 4 expression induced by high glucose level exposure. Deletion of DUSP4 exacerbated albuminuria and increased mesangial expansion and glomerular fibrosis in diabetic mice. These morphological changes were associated with profound podocyte foot process effacement, cell death, and sustained p38 and JNK activation. Moreover, inhibition of protein kinase C-δ prevented DUSP4 expression decline and p38/JNK activation in the podocytes and renal cortex of diabetic mice. Analysis of DUSP4 expression in the renal cortex of patients with diabetes revealed that decreased DUSP4 mRNA expression correlated with reduced estimated glomerular filtration rate (<60 mL/min/1.73 m^2). Thus, this study demonstrates that preserving DUSP4 expression could protect against podocyte dysfunction and preserve glomerular function in DN.

Diabetic nephropathy (DN) is a microvascular complication of diabetes that ultimately evolves to end-stage renal disease (1). Ample evidence has shown that the glomerular podocytes are affected early in the onset of DN and heavily contribute to the loss of filtration slit found in the glomeruli (2,3). Clinical studies reported that the reduction of podocyte number and density is one of the strongest predictors of DN progression (4). We and others have demonstrated that hyperglycemia enhanced podocyte cell death (5,6). However, the exact cellular mechanisms driven by high glucose (HG) that contribute to podocyte loss are yet to be fully elucidated.

Activation of mitogen-activated protein kinases (MAPKs) by hyperglycemia has been linked to multiple cellular disorders (7–10). Enhanced activity of c-Jun N-terminal kinase (JNK) in the liver, fat, and muscle tissues of *ob/ob* mice is associated with insulin resistance (8). Activation of p38 by HG levels is involved in smooth muscle and retinal pericytes cell death (9). In the kidney, histological analyses indicated that p38 is chronically activated in the glomerulus of rodent models of DN and in patients with type 2 diabetes (11–13), whereas inhibition of p38 activity in diabetic normotensive rats reduced albuminuria and prevented the increased expression of fibronectin (14). Another study showed that inhibition of apoptosis signal-regulating kinase 1 (ASK1), a kinase upstream of p38, prevented glomerulosclerosis, reduced inflammation, and improved renal function in diabetic endothelial nitric oxide synthase–knockout mice (15). In podocytes, Mima et al. (6) reported that HG level exposure raised the activation of p38α, which caused cell death, an effect that could be prevented with a specific p38 inhibitor. Although inhibition of MAPK has been a successful avenue to alter the development of renal pathology in rodent models of

[1]Research Center of the CHU de Sherbrooke, Université de Sherbrooke, Sherbrooke, Québec, Canada
[2]Division of Cardiology, Department of Medicine, Université de Sherbrooke, Sherbrooke, Québec, Canada
[3]Division of Nephrology, Department of Medicine, Université de Sherbrooke, Sherbrooke, Québec, Canada
[4]Division of Endocrinology, Department of Medicine, Université de Sherbrooke, Sherbrooke, Québec, Canada

Corresponding author: Pedro Geraldes, pedro.geraldes@usherbrooke.ca

Received 1 August 2018 and accepted 25 February 2019

This article contains Supplementary Data online at http://diabetes.diabetesjournals.org/lookup/suppl/doi:10.2337/db18-0837/-/DC1.

DN, treatment with a MAPK inhibitor in clinical human trials caused secondary effects (16), suggesting that new strategies to prevent their activation in diabetes are critically needed.

Dual specificity phosphatase (DUSP) proteins are a large family of serine/threonine and tyrosine phosphatases, some of which are referred as MAPK phosphatases because they directly bind to activated MAPKs and cause their inhibition (17,18). Genetic deletion of DUSP in mice models uncovered their role in the regulation of various metabolic pathways (19–22). In the heart, mice with double-knockout of DUSP1 and DUSP4 showed hypertrophy of cardiomyocytes, which is associated with sustained p38 activation (23). Ablation of DUSP1 enhanced nuclear activity of extracellular signal–regulated kinase (ERK), p38, and JNK, rendering mice resistant to diet-induced obesity (21).

The exact mechanisms leading to MAPK activation in DN are not fully understood. Because DUSPs are the major mechanism of inhibition of MAPK in mammalian cells (24), we hypothesized that diabetes deregulates DUSP expression in podocytes, which contributes to their cellular dysfunction and progression of DN.

RESEARCH DESIGN AND METHODS

Reagents and Antibodies

Primary antibodies for immunoblotting and immunochemistry were obtained from commercial sources, including actin (horseradish peroxidase conjugated; I-19), DUSP4 (S-18), phosphorylated (p)-JNK (G-7), JNK (D-2), BAX (N-20), and WT-1 (C-19) from Santa Cruz Biotechnology (Santa Cruz, CA); p38 MAPK (9212), p-p38 MAPK (D3F9), ERK, p-ERK (D13.14.4E), and protein kinase C (PKC)-δ (2058) from Cell Signaling (Beverly, MA); collagen type IV (Col IV; Novus Biological, Littleton, CO), Alexa 546–conjugated anti-rabbit from Jackson ImmunoResearch Laboratories (West Grove, PA), and Alexa Fluor 594–conjugated anti-mouse from Invitrogen (Carlsbad, CA). All other reagents used, including RPMI-1640, EDTA, leupeptin, phenylmethyl-sulfonyl fluoride, aprotinin, D-glucose, D-mannitol, FITC-inulin, and Na_3VO_4 were purchased from MilliporeSigma (Oakville, Ontario, Canada), FBS was purchased from Wisent Bioproducts (Saint-Jean-Baptiste, Québec, Canada), and penicillin-streptomycin was obtained from Invitrogen.

Animals and Experimental Design

C57BL/6J (*Ins2*$^{+/+}$), diabetic heterozygous male *Ins2*$^{+/C96Y}$ (Akita) and DUSP4 knockout (*Dusp4*$^{-/-}$) mice were purchased from The Jackson Laboratory and bred in our animal facility for seven generations. Male *Ins2*$^{+/C96Y}$*Dusp4*$^{+/-}$ were bred with female *Ins2*$^{+/+}$*Dusp4*$^{+/-}$ mice. The Akita mice develop hyperglycemia, hypoinsulinemia, polydipsia, and polyuria caused by a misfolding of the insulin protein, beginning at ~3–4 weeks of age. These mice were sacrificed after 6 months of diabetes. *Prkcd*$^{-/-}$ mice were generated by inserting a LacZ/neo cassette into the first transcribed exon of the PKC-δ gene as described previously (25). *Prkcd*$^{-/-}$ mice were rendered diabetic for a 6-month period by an intraperitoneal streptozotocin injection (50 mg/kg in 0.1 mol/L citrate buffer, pH 4.5) (MilliporeSigma) on 5 consecutive days after an overnight fast; control mice were injected with citrate buffer. Throughout the period of study, animals were provided with free access to water and standard rodent chow (Harlan Teklad). All experiments were conducted in accordance with the Canadian Council of Animal Care and Institutional Guidelines and were approved by the University of Sherbrooke Animal Care and Use Committees according to National Institutes of Health guidelines.

Blood Glucose, Insulin Levels, Urinary Albumin, and 8-Isoprostane Excretion and Glomerular Filtration Rate Measurements

Blood glucose was measured by a Contour glucometer (Bayer, Pointe-Claire, Québec, Canada). Insulin levels were measured using the commercial ultrasensitive mouse insulin ELISA kit from Crystal Chem (Elk Grove Village, IL). A 24-h urine collection was obtained from each mouse the day before the sacrifice in individual mouse metabolic cages (Nalgene Nunc International, Rochester, NY) with free access to water and rodent mash. Urinary albumin levels were measured using an indirect competitive ELISA according to the manufacturer's instructions (Albuwell M; Exocell, Philadelphia, PA). Urinary 8-isoprostane levels were measured using a competitive ELISA assay according to the manufacturer's instructions (8-isoprostane EIA kit; Cayman Chemical, Ann Arbor, MI). The glomerular filtration rate (GFR) was evaluated using FITC-inulin clearance as we previously described (26).

Blood Pressure Measurements

Systolic blood pressure (BP) and mean arterial pressure were measured on conscious animals using the CODA tail-cuff system (Kent Scientific, Torrington, CT). Briefly, animals were acclimated on the machine for 3 consecutive days, and data were collected on the 4th day. Measurements consisted of 25 cycles, of which the first and last 5 cycles were discarded. The average of at least five consecutive measurement considered "true" by the machine were used to evaluate BP of the animal.

Tissue Preparation and Transmission Electron Microscopy

Right mouse kidneys were harvested for pathological examination, and sections were fixed in 4% paraformaldehyde (MilliporeSigma) and then transferred to 70% ethanol for immunohistochemistry. The tissue was embedded in paraffin, and 4-μm sections were stained with periodic acid Schiff and Masson trichome (MilliporeSigma). Left mouse kidneys were used for transmission and scanning electron microscopy to evaluate podocyte structure and foot process effacement, as previously described (26). Fifteen glomerular tufts per animal were chosen randomly for analysis.

Immunofluorescence

Left mouse kidneys were directly frozen in optimal cutting temperature embedding compound (Sakura Fintech USA, Torrance, CA) in cryomolds on a block of dry ice and sectioned at 6 μm (Leica Cryostat). Immunofluorescence of the section using WT1 (1:50) (SC-192, Santa Cruz), p-p38 (1:50) (28B10, Cell Signaling), nephrin GP-N2 from PROGEN Biotechnik (1:50), and DUSP4 (1:50) (ab216576, Abcam) were performed as previously described (26). Images of one experiment were taken at the same time under identical settings and handled similarly in Adobe Photoshop across all images.

Immunohistochemistry

Immunochemistry of kidney sections was performed using the ABC kit (Vector Laboratories, Burlington, Ontario, Canada), according to the manufacturer's protocol. Coloration was obtained by incubating sections in diaminobenzidine solution (Vector Laboratories). Counterstaining of the nucleus was done using Gill's formula hematoxylin (Vector Laboratories).

Mesangium Expansion, Glomerular Hypertrophy, and Quantitation of Podocyte Cell Death

Mesangial matrix expansion and glomerular hypertrophy were measured as we previously described (5). Apoptotic nuclei of kidney sections were detected using the TACS 2 Tdt-Fluor in situ apoptosis detection kit (Trevigen, Gaithersburg, MD) according to the manufacturer's instructions and as we previously described (5). Podocytes were counted as cell death when both podocyte marker and Tdt-fluorescein–positive cells colocalized. A total of 20–30 glomeruli were evaluated on the transverse section of the left kidney.

Isolation of the Glomeruli and Tubules

Renal cortices of two kidneys (one per mouse) were combined, minced, and all the tissue was passed through a 200-, 150-, 75-, and 40-μm sieve. The glomeruli remained at the top of the 75-μm sieve, whereas the tubular cells remained at the top of 40-μm sieve. Each fraction was collected with PBS and centrifuged for 10 min at 500*g*. The glomeruli and tubule samples (two kidneys per *N*, total of $N = 5$ per group) were then used for mRNA analyses.

Cell Culture and Adenoviral Vector Transfection

A well-characterized mouse podocyte cell line was obtained from Dr. Saleem's group (27) and cultured as previously described. After differentiation of podocytes for 14 days, medium was changed to RPMI 0.1% FBS containing normal glucose (NG; 5.6 mmol/L + 19.4 mmol/L mannitol to adjust osmotic pressure) or HG (25 mmol/L) up to 96 h. Adenoviral vectors containing green fluorescent protein (GFP, Ad-GFP), wild-type form of DUSP4, and dominant negative of PKC-δ were used to infect podocytes, as we reported previously (26).

Real-time PCR Analyses

Real-time PCR was performed to evaluate mRNA expressions of DUSP1, DUSP4, DUSP6, DUSP10, NADPH oxidase 4 (NOX4), heme oxygenase isozyme 1 (HO-1), Col IV, transforming growth factor-β (TGF-β), and fibronectin, as previously described (26). PCR primers are listed in Supplementary Table 1. GAPDH mRNA expression was used for normalization.

Caspase 3/7 Assay

Caspase 3 and 7 enzymatic activities were determined by quantification of cleaved substrate using the luminescent assay Caspase 3/7 Glo (Promega, Madison, WI), as previously described (5).

Measurement of Cellular Oxidative Stress

Measurement of cellular oxidative stress was performed using CellROX deep red reagent (Invitrogen) according to the manufacturer's instructions. Briefly, CellROX was added to cell media at a final concentration of 5 μmol/L for 30 min. Cells were washed three times with PBS, and fluorescence was measured (640/665 absorption/emission) using a fluorescent plate reader. Specificity of the fluorescent signal was confirmed podocytes exposed to H_2O_2 (as positive control) and *N*-acetylcysteine (as negative control).

Human Tissue Study

After written consent, kidney tissue was obtained from eight patients with diabetic kidney disease at the time of nephrectomy for conventional renal carcinoma. Baseline characteristics of the patients are listed in Supplementary Table 2. A pathologist masked to the study groups performed all histological analyses. To assess renal function, the Chronic Kidney Disease Epidemiology Collaboration formula was used for the estimated GFR (eGFR) (28). Serum creatinine was obtained within 1 month before the surgery. The urine sample was sent to the laboratory where it was centrifuged and tested for urinary albumin (by immunoturbidimetric method) and creatinine (by enzymatic method). The albumin-to-creatinine ratio was calculated. DUSP1 and DUSP4 mRNA levels were measured from the renal cortex of patients with diabetes by quantitative PCR as described above. Phosphorylation levels of p38 and JNK and DUSP4 protein expression were measured by immunoblot experiments as described above. The study was approved by the Centre Intégré Universitaire de Santé et de Services Sociaux de l'Estrie–CHU de Sherbrooke Research Ethics Board and was conducted in accordance with the Declaration of Helsinki.

Statistical Analyses

In vitro and in vivo data are shown as mean ± SD for each group. Statistical analysis was performed by unpaired *t* test or by one-way ANOVA, followed by the Tukey test correction for multiple comparisons. Data in each group were checked for normal distribution using the D'Agostino and

Pearson normality test based on $\alpha = 0.05$. All results were considered statistically significant at $P < 0.05$. Correlation of the data obtained from human patients was verified with the Spearman ρ correlation test. The association between two variables was considered statistically significant at $P < 0.05$.

RESULTS

HG-Induced Activation of p38 and JNK in Podocytes Is Associated With Reduced DUSP4 Expression

Expression levels of p38 and JNK phosphorylation were increased by 2.05- and 2.08-fold, respectively, while phosphorylation of ERK did not change (Fig. 1*A*). Because DUSPs are involved in the regulation of MAPK activity, we assessed the expression levels of DUSP known to inhibit p38 and JNK. DUSP4 mRNA (Fig. 1*B*) and protein (Fig. 1*C*) expression were significantly reduced in podocytes exposed to HG levels compared with NG levels, while the expression of the mRNA of other DUSPs remained unchanged (Fig. 1*B*). Interestingly, although p38 MAPK was activated in mesangial cells cultured in HG media, the expression of DUSP4 was not affected in these cells (data not shown).

Overexpression of DUSP4 Prevented HG Level-Induced p38, JNK, Caspase 3/7, BAX, and NOX4

To investigate the relative role of DUSP4, we used adenoviral vectors to overexpress the native form of DUSP4. In GFP-overexpressed podocytes, HG level exposure raised the phosphorylation of p38 and JNK as expected. In contrast, overexpression of DUSP4 prevented p38 and JNK activity caused by HG level exposure, without affecting the phosphorylation of ERK in both NG and HG conditions (Fig. 2*A*). The overexpression of DUSP4 did not influence the expression of other DUSP transcripts (Fig. 2*B*). Podocytes exposed to HG levels exhibited elevated enzymatic activity of caspase 3/7 (Fig. 2*C*) and BAX expression (Fig. 2*D*), a protein involved in cell death (29,30), compared with NG levels. These effects were prevented by the overexpression of DUSP4 in HG conditions (Fig. 2*C* and *D*). Since oxidative stress generation has been proposed as one potential mechanism for podocyte cell death caused by chronic exposure of HG levels, we measured NOX4, HO-1, and superoxide production as a marker of oxidative stress. Our results indicated that HG concentrations increased NOX4 (Fig. 2*E*), HO-1 (Supplementary Fig. 1*A*) mRNA expression, and superoxide production (Supplementary Fig. 1*B*) that were attenuated in podocytes with overexpression of DUSP4 (Fig. 2*E* and Supplementary Fig. 1*A* and *B*).

PKC-δ Activation by HG Is Responsible for the Loss of DUSP4 in Podocytes

We and others have reported that HG levels lead to activation of PKC-δ in cultured podocytes (5,6). Since PKC-δ activation has been shown to decrease DUSP1

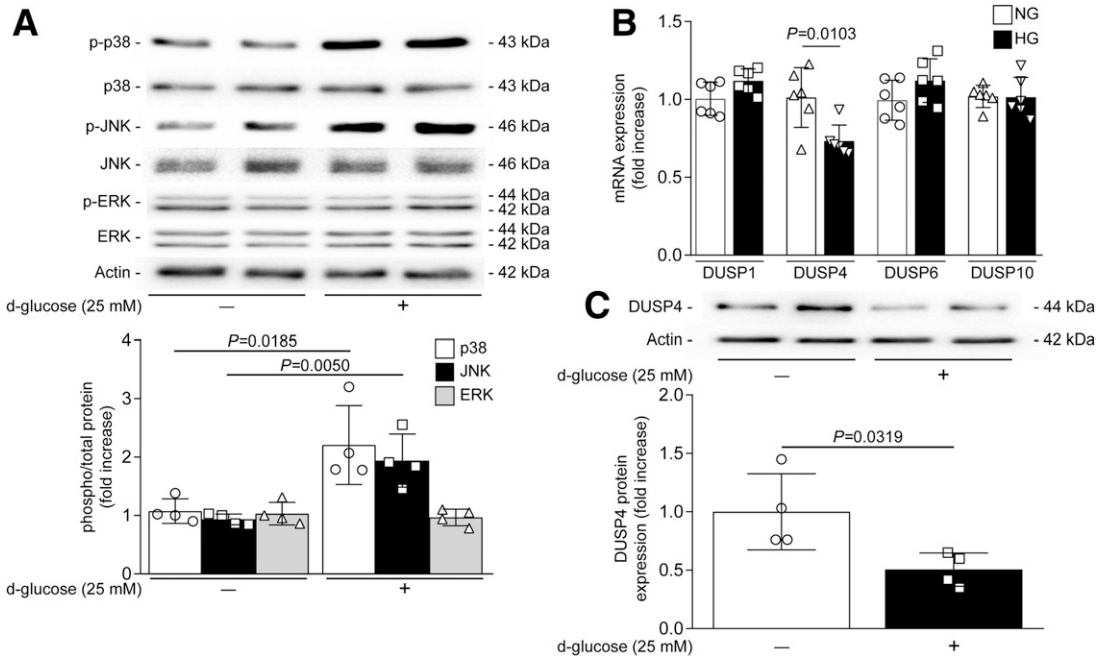

Figure 1—HG induces activation of p38 and JNK and is associated with reduced DUSP4 expression. Podocytes were exposed to NG (5.6 mmol/L glucose + 19.4 mmol/L mannitol) or HG (25 mmol/L glucose) for 72 h. *A*: Expression of p-p38, p38, p-JNK, JNK, p-ERK, ERK, and actin was detected by immunoblot, and densitometry quantitation was measured. DUSP1, DUSP6, DUSP10, and DUSP4 mRNA (*B*) and protein (*C*) expression were measured by quantitative PCR and immunoblot analyses. Results are shown as mean ± SD of four (*A* and *C*) and six (*B*) independent experiments.

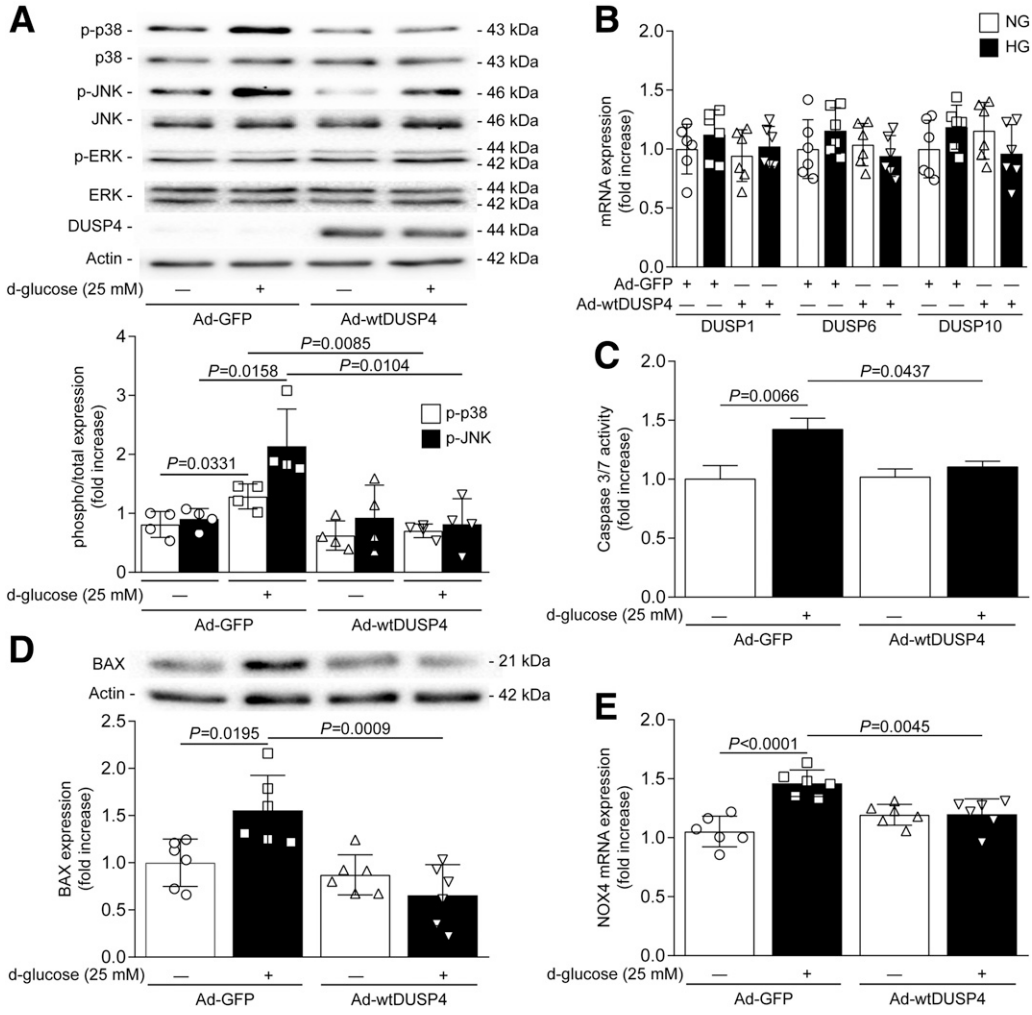

Figure 2—Overexpression of DUSP4 prevents HG-induced activation of p38, JNK, caspase 3/7 activity, and BAX expression. Podocytes were infected with Ad-GFP or adenovirus containing wild-type DUSP4 (Ad-wtDUSP4) before being exposed to NG or HG for 72 h. Expression of p-p38, p38, p-JNK, JNK, p-ERK, ERK, and DUSP4 (*A*) and of BAX and actin (*D*) was detected by immunoblot, and densitometry quantitation was measured. DUSP1, DUSP4, DUSP6, DUSP10 (*B*), and NOX4 (*E*) mRNA expression was quantified by quantitative PCR. *C*: Caspase 3/7 enzymatic activity was measured according to the manufacturer's instructions. Results are shown as mean ± SD of 4 (*A*), 6 (*B*, *D*, and *E*), and 12 (*C*) independent experiments.

expression (31,32), we evaluated the effect of overexpression of the dominant negative form of PKC-δ on DUSP4 expression. Whereas DUSP4 expression was reduced by 30% in podocytes exposed to HG concentrations, overexpression of the dominant negative form of PKC-δ significantly restored DUSP4 mRNA (Fig. 3*A*) and protein (Fig. 3*B*) expression in HG conditions similar to NG conditions. The dominant negative form had no effect on other DUSP expression (Supplementary Fig. 2). Overexpression of the dominant negative form of PKC-δ also prevented HG-induced phosphorylation of p38 and JNK (Fig. 3*C*). Previous data indicated that PKC activation can raise oxidant stress signals and that increased NOX4 expression is an important contributor of this process in podocytes (33). Therefore, regulation of NOX4 expression by PKC-δ in podocytes was assessed. As expected, NOX4 expression levels were significantly increased by 42% in podocytes exposed to HG levels. Interestingly, overexpression of the dominant negative form of PKC-δ prevented the HG-induced elevated expression of NOX4 in podocytes (Fig. 3*D*).

DUSP4 Expression Is Reduced in the Renal Glomeruli of Type 1 Diabetic Mice

It is well recognized that stress-induced MAPKs are activated in the kidney of diabetic mice (13,34–36). Our data corroborated previous observations that phosphorylation of p38 and JNK, but not ERK, was significantly elevated in the renal cortex (Fig. 4*A*) and glomerular podocytes (Fig. 4*B*) of 7-month-old diabetic *Ins2*$^{+/C96Y}$ mice compared with their nondiabetic *Ins2*$^{+/+}$ littermate controls. Since p38 and JNK activation can be regulated by DUSPs, mRNA expression of DUSP1, DUSP4, DUSP6, and DUSP10 was evaluated. Our data demonstrated that the expression levels of

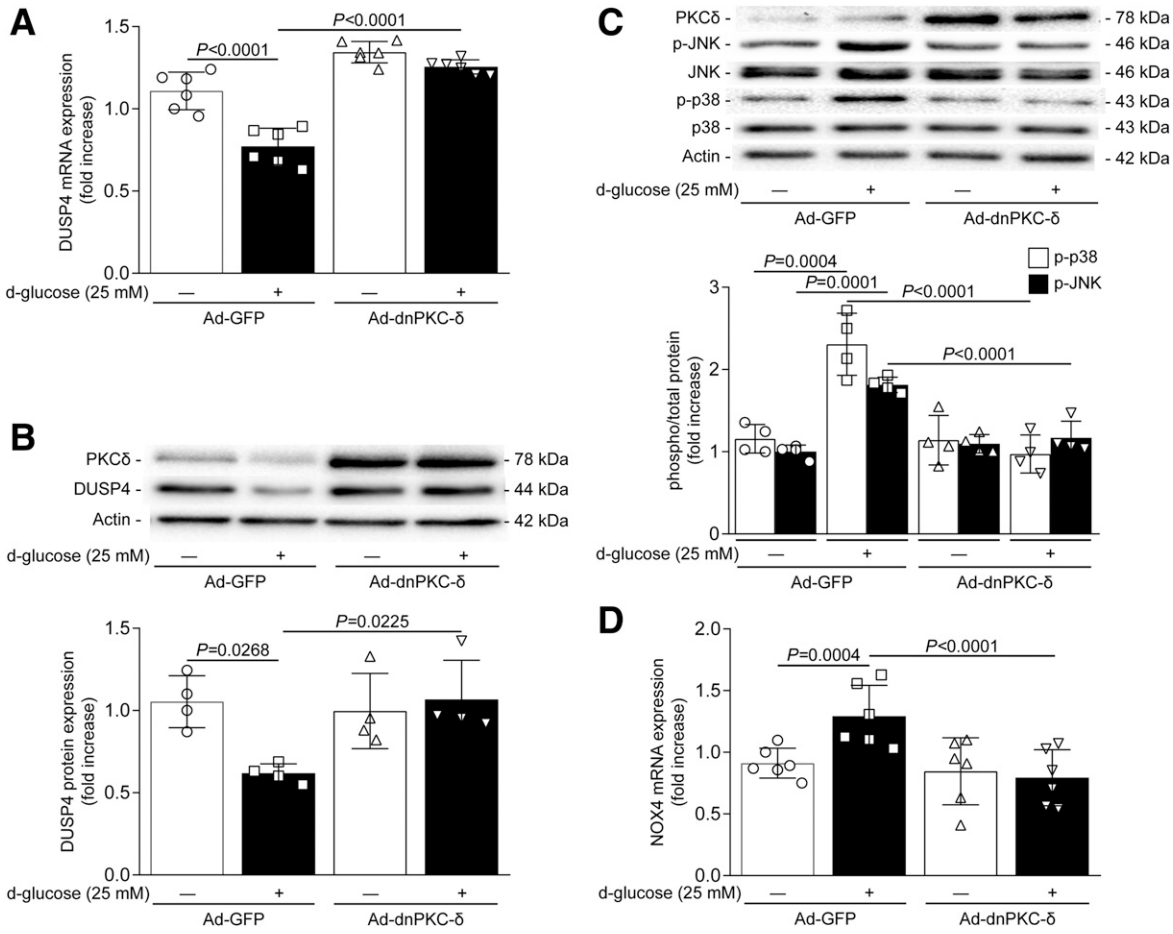

Figure 3—PKC-δ activity promotes loss of DUSP4 expression and activation of p38, JNK, and NOX4 in the HG condition. Podocytes were infected with Ad-GFP or adenovirus containing dominant negative PKC-δ (Ad-dnPKC-δ) before being exposed to NG or HG for 72 h. Expression of DUSP4 (*A*), p-p38, p38, p-JNK, JNK, PKC- δ, and actin (*B*) was detected by immunoblot, and densitometry quantitation was measured. DUSP4 protein (*B*) and NOX4 mRNA (*D*) expression were evaluated by quantitative PCR. Results are shown as mean ± SD of six (*A* and *D*) and four (*B* and *C*) independent experiments.

DUSP4 were significantly decreased by 50% (P = 0.001) in the renal cortex of diabetic mice compared with nondiabetic mice, whereas the expression of the other DUSPs remained unchanged (Fig. 4*C*). Because the renal cortex contains many cell types, we isolated glomeruli and tubules from all groups of mice. As indicated in Fig. 4*D* and *E*, DUSP4 mRNA expression was significantly reduced in both glomerular podocytes and tubules of diabetic $Ins2^{+/C96Y}$ mice compared with nondiabetic $Ins2^{+/+}$ mice.

Deletion of DUSP4 in Diabetic Mice Increased Urinary Albumin Levels

To define the role of DUSP4 in the kidney, we generated type 1 diabetic mice ($Ins2^{+/C96Y}$) that do not possess the gene coding for DUSP4 ($Dusp4^{-/-}$). Body weight and systemic glucose and insulin levels were not different between diabetic $Ins2^{+/C96Y}$ and diabetic $Ins2^{+/C96Y}$ $Dusp4^{-/-}$ mice at 5 and 7 months of age (Supplementary Table 3). Urinary albumin levels were increased by 2.8-fold in diabetic $Ins2^{+/C96Y}$ mice compared with nondiabetic $Ins2^{+/+}$ mice (Fig. 5*A*). Interestingly, diabetic $Ins2^{+/C96Y}Dusp4^{-/-}$ showed a significant increase in urinary albumin levels, with a 3.5-fold increase ($P < 0.0001$) compared with diabetic $Ins2^{+/C96Y}$ mice, suggesting that deletion of DUSP4 exacerbated renal damage in diabetic mice (Fig. 5*A*). As expected, GFR (Fig. 5*B*) and BP (Fig. 5*C* and *D*) were significantly increased in diabetic $Ins2^{+/C96Y}$ mice compared with nondiabetic $Ins2^{+/+}$ mice. The absence of DUSP4 in diabetic $Ins2^{+/C96Y}$ mice had no additional effect on GFR and BP compared with diabetic $Dusp4^{+/+}$ mice (Fig. 5*B–D*).

Low GFR Levels in Patients With Diabetes Are Associated With Reduced DUSP4 Expression

To assess the potential role of DUSP4 in the development of DN, we evaluated in humans with confirmed diabetic glomerulosclerosis on kidney histology whether low DUSP4 expression could be associated with reduced renal function. DUSP4 mRNA levels were extracted from the renal cortex of eight patients with diabetes. Our data demonstrated that reduced DUSP4 mRNA expression in renal tissue of patients with diabetes was strongly correlated with reduced eGFR (R^2 = 0.714; P = 0.047)

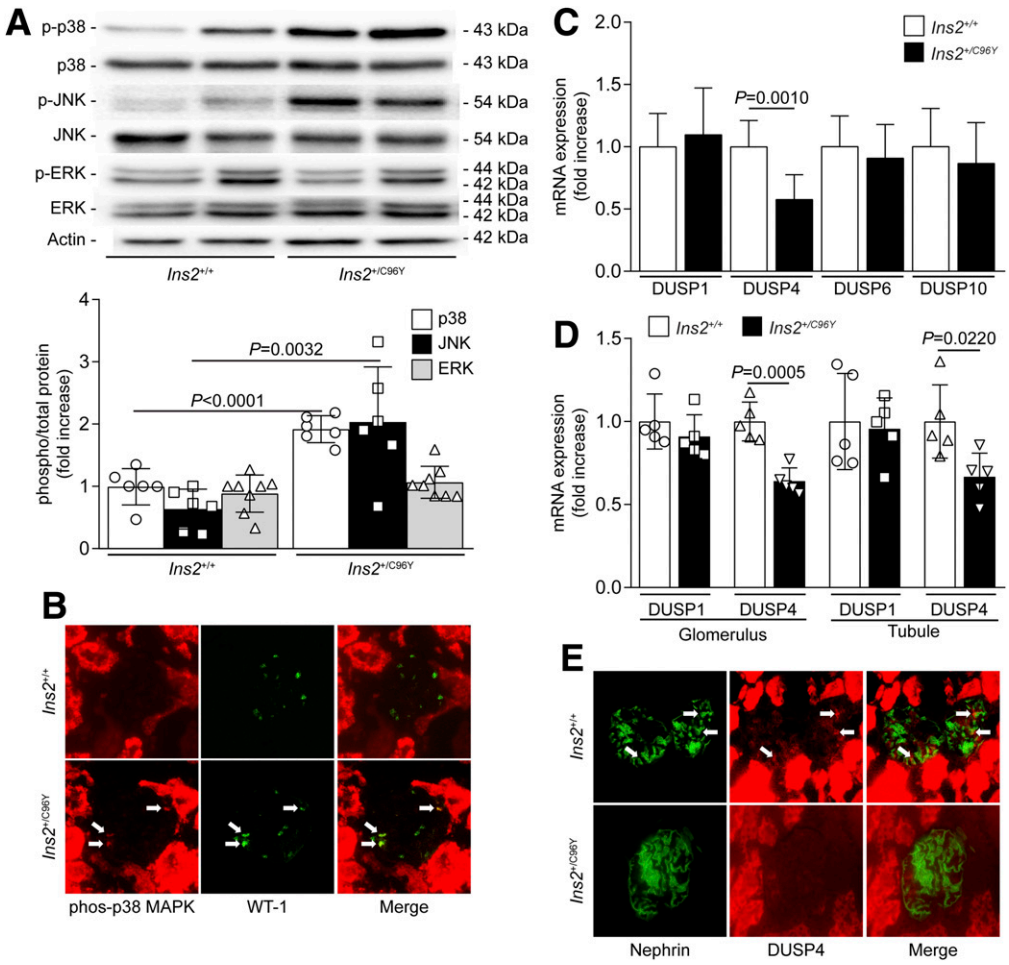

Figure 4—Activation of MAPK and DUSP expression in the renal cortex of *Ins2*$^{+/C96Y}$ mice. Expression of p38, JNK, and ERK phosphorylation in extracted protein lysate (*A*) and cross-sections of the renal cortex (*B*) of 7-month-old *Ins2*$^{+/+}$ and *Ins2*$^{+/C96Y}$ mice. Expression of various DUSPs from the renal cortex (*C*) and glomeruli and tubules (*D*) was evaluated by quantitative PCR experiments, and by immunofluorescence analysis (*E*). Arrows represent activated p-38 MAPK (*B*) and DUSP4 expression positive podocytes (using WT-1 and nephrin as podocyte markers) (*E*). Results are shown as mean ± SD of six (*A*, *B*, and *E*), eight (*C*), and five (*D*, with each *N* included one kidney of two mice) mice per group.

(Fig. 5*E*). Interestingly, DUSP4 mRNA expression levels decreased significantly between patients without diabetes with normal renal function and patients with diabetes with eGFR <60 mL/min/1.73 m^2 (P = 0.0249) and slightly reduced (not significantly) compared with patients with diabetes with GFR >60 mL/min/1.73 m^2 (Fig. 5*F*). More importantly, immunoblot experiments corroborated the association between eGFR levels, DUSP4 protein expression, and activation of p38 and JNK MAPK (Fig. 5*G*). In contrast, no correlation was observed between DUSP1 mRNA expression and eGFR (Supplementary Fig. 3) and DUSP4 mRNA expression and the albumin-to-creatinine ratio (Supplementary Fig. 4).

Glomerular Pathology Is Worsened in Diabetic Mice With Deletion of DUSP4

We and others have shown that diabetic *Ins2*$^{+/C96Y}$ mice exhibited glomerular pathology similar to DN (5,37). As expected, glomerular hypertrophy and mesangial expansion are elevated in diabetic *Ins2*$^{+/C96Y}$ mice compared with nondiabetic *Ins2*$^{+/+}$ mice (Fig. 6*A*–*C*). Diabetic *Ins2*$^{+/C96Y}$*Dusp4*$^{-/-}$ mice showed no change in glomerular size compared with diabetic *Ins2*$^{+/C96Y}$ mice, while mesangial expansion was significantly increased. Masson trichrome staining was performed to evaluate glomerular fibrosis, a characteristic of chronic kidney disease. Nondiabetic *Ins2*$^{+/+}$ and *Ins2*$^{+/+}$*Dusp4*$^{-/-}$ mice were free of fibrosis (blue staining) in their glomerulus, whereas diabetic *Ins2*$^{+/C96Y}$ mice showed slight peripheral glomerular fibrosis. In stark contrast, diabetic *Ins2*$^{+/C96Y}$*Dusp4*$^{-/-}$ mice exhibited heavy fibrosis expression in their glomeruli ($P <$ 0.0001) (Fig. 6*D* and *E*). Increased appearance of fibrosis was associated with elevated Col IV staining in the glomeruli of diabetic *Ins2*$^{+/C96Y}$*Dusp4*$^{-/-}$ compared with diabetic *Ins2*$^{+/C96Y}$ mice (Fig. 6*F* and *G*). To corroborate the presence of fibrosis in the glomeruli, diabetic *Ins2*$^{+/C96Y}$*Dusp4*$^{-/-}$ mice exhibited elevated mRNA expression of Col IV, fibronectin, and TGF-β compared with diabetic *Ins2*$^{+/C96Y}$ mice (Fig. 6*H*–*J*).

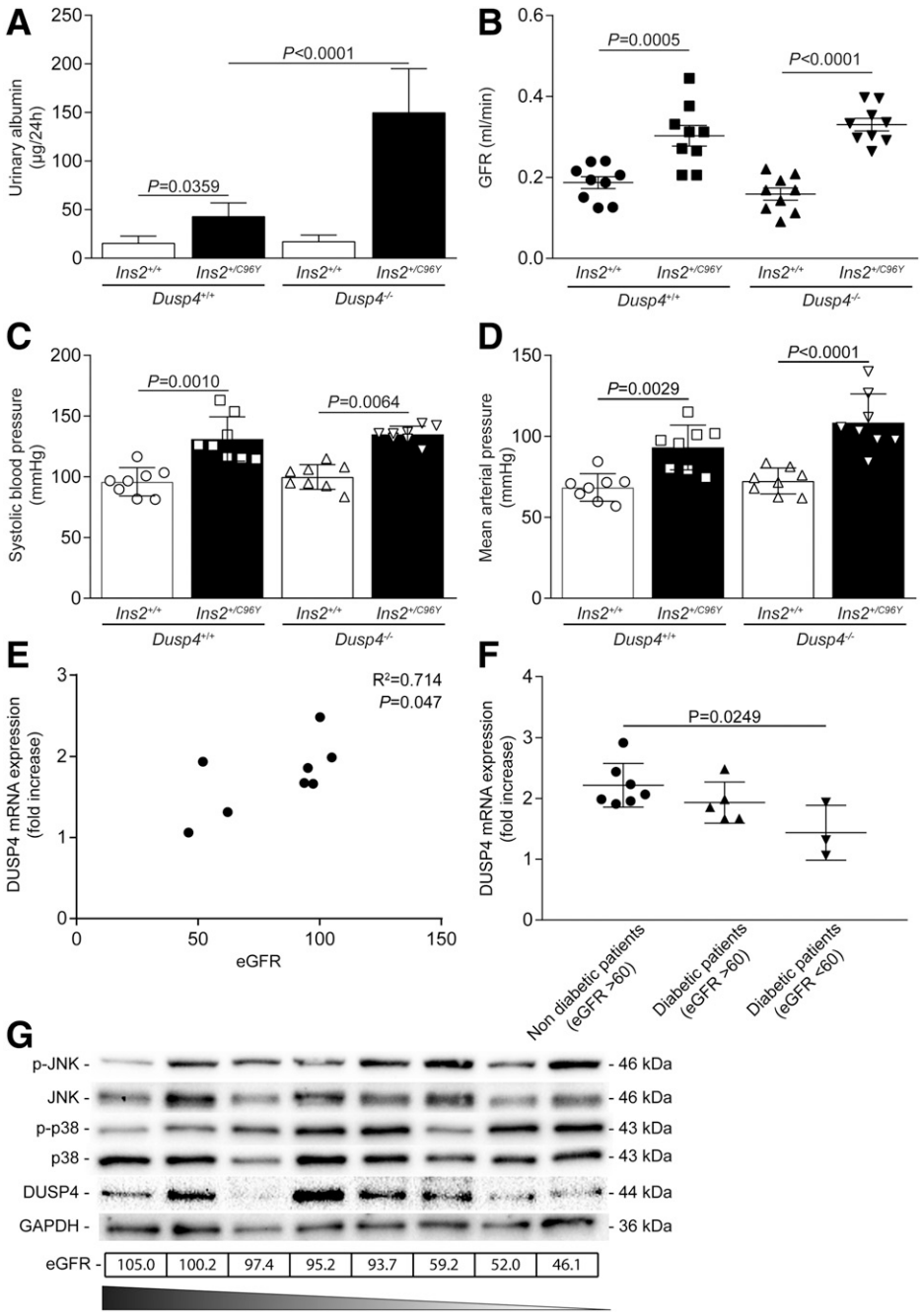

Figure 5—Renal dysfunction, BP, and metabolic parameters of *Ins2*$^{+/C96Y}$ and *Dusp4*$^{-/-}$ mice and patients with diabetes. Urinary albumin levels (*A*), GFR (*B*), systolic BP (*C*), and mean arterial pressure (*D*) were measured in 7-month-old *Ins2*$^{+/+}$ and *Ins2*$^{+/C96Y}$ mice with deletion of *Dusp4* gene (*Dusp4*$^{-/-}$). Results are shown as mean ± SD of 12 (*A*), 9 (*B*), and 8 (*C* and *D*) mice per group. *E* and *F*: DUSP4 mRNA expression of the renal cortex of patients with (n = 8) and without (n = 7) diabetes who underwent nephrectomy was measured by quantitative PCR. eGFR was evaluated by serum creatinine measurements using the Chronic Kidney Disease Epidemiology Collaboration formula. *G*: Expression of p-p38, p38, p-JNK, JNK, DUSP4, and GAPDH in protein lysate extracted from renal cortex of patients with diabetes (n = 8) was detected by immunoblot.

Deletion of DUSP4 in Diabetic Mice Exacerbates Podocyte Foot Process Effacement, Loss of Slit Diaphragm, and Cell Death

Since podocytes are an essential component of this barrier, we evaluated podocyte integrity using scanning and transmission electron microscopy. Diabetic *Ins2*$^{+/C96Y}$ mice showed areas with foot process effacement and loss of filtration slit. Interestingly, diabetic *Ins2*$^{+/C96Y}$*Dusp4*$^{-/-}$ mice exhibited profound and severe podocyte damage, with multiple areas with heavy foot process effacement and large region of loss of filtration slit (Fig. 7*A*–*C*). We have reported that podocyte cell death is elevated in

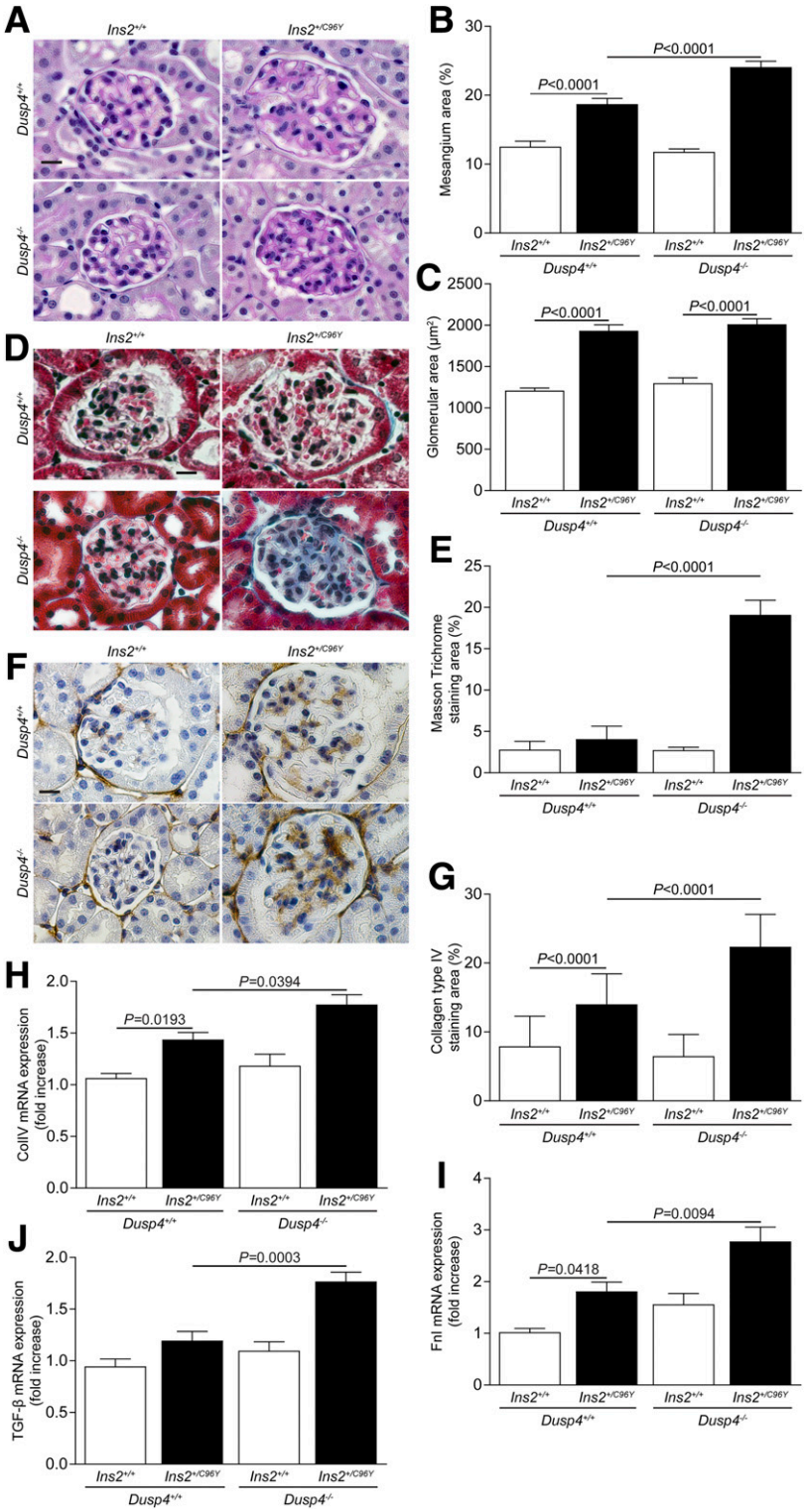

Figure 6— Renal pathology and glomerular fibrosis of *Ins2*$^{+/C96Y}$ and *Dusp4*$^{-/-}$ mice. Renal cross-sections of 7-month-old mice were stained with periodic acid Schiff (*A*) to quantify mesangial expansion (*B*) and glomerular size (*C*), and with Masson trichrome (*D*) to quantify glomerular fibrosis (*E*). *F* and *G*: Immunohistochemistry using antibody against Col IV was quantified. mRNA expression of Col IV (*H*), fibronectin (*I*), and TGF-β (*J*) was measured by quantitative PCR. Results are shown as mean ± SD of six to eight glomeruli of six (*A*–*G*) and eight (*H*–*I*) mice per group. Scale bars = 10 μm.

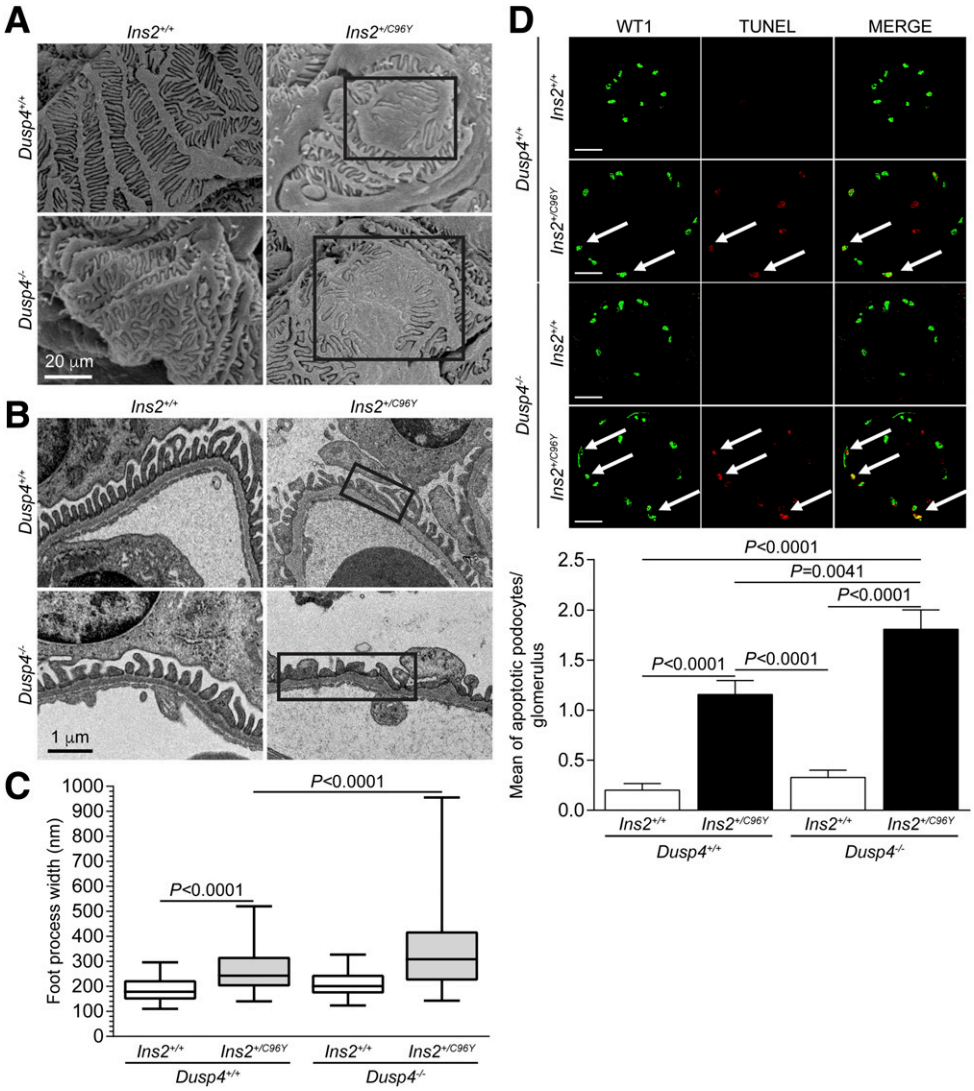

Figure 7—Foot process effacement and podocyte cell death in *Ins2*$^{+/C96Y}$*Dusp4*$^{-/-}$ mice. Transmission electron microscopy (*A*) and scanning electron microscopy (*B*) of podocyte foot process structure, and quantification (*C*). *D*: Immunofluorescence of podocyte nucleus (WT1; green) and apoptotic-positive cells (TUNEL; red) in the glomerulus of *Ins2*$^{+/+}$, *Ins2*$^{+/C96Y}$, *Ins2*$^{+/+}$*Dusp4*$^{-/-}$, and *Ins2*$^{+/C96Y}$*Dusp4*$^{-/-}$ mice. Scale bars = 10 μm. Arrows represent colocalization of podocyte and apoptotic markers. Boxes (*A* and *B*) represent podocyte effacement process. Results are shown as mean ± SD of eight glomeruli of six mice per group (*A*, *B*, and *D*) and four mice per group with a minimum of 50 measurements per mouse (*C*).

diabetic *Ins2*$^{+/C96Y}$ mice compared with their nondiabetic counterparts (5). Using the same technique, we confirmed the increase of podocytes cell death signal per glomerulus in diabetic *Ins2*$^{+/C96Y}$ mice compared with nondiabetic *Ins2*$^{+/+}$ mice. The number of podocytes positive for cell death was significantly enhanced in diabetic *Ins2*$^{+/+}$*Dusp4*$^{-/-}$ mice compared with diabetic *Ins2*$^{+/C96Y}$ mice (Fig. 7*D*).

PKC-δ–Induced Loss of DUSP4 Expression in Diabetic Mice Causes Activation of p38 and JNK MAPK, Increased BAX Expression, and Oxidant Production

To verify whether PKC-δ activation in vivo could be linked to reduced DUSP4 expression in diabetic mice, we measured mRNA expression of DUSP4 in nondiabetic and diabetic mice with or without deletion of PKC-δ (*Prkcd*$^{-/-}$). DUSP4 mRNA levels were significantly decreased by 45% in the renal cortex of diabetic mice. Deletion of PKC-δ prevented both diabetes-induced reduction of DUSP4 expression (Fig. 8*A*) and increased phosphorylation levels of p38 and JNK (Fig. 8*B* and *C*). Both p38 and JNK MAPK phosphorylation were also significantly increased in diabetic *Ins2*$^{+/C96Y}$ mice compared with nondiabetic *Ins2*$^{+/+}$ mice (Fig. 8*D*). In contrast to diabetic *Prkcd*$^{-/-}$ mice, phosphorylation levels of p38 and JNK MAPK were further enhanced in diabetic *Ins2*$^{+/C96Y}$*Dusp4*$^{-/-}$ mice compared with diabetic *Ins2*$^{+/C96Y}$ mice, whereas ERK phosphorylation levels did not change by the absence of DUSP4 (Fig. 8*D*). Elevated levels of p38 and JNK phosphorylation in diabetic *Ins2*$^{+/C96Y}$*Dusp4*$^{-/-}$ mice were associated with a remarkable sevenfold increase of the expression of the proapoptotic

protein BAX (Fig. 8*E*). Since our cultured podocyte data showed that DUSP4 overexpression prevented NOX4 expression, we measured urinary 8-isoprostane, a marker of oxidative stress production. Levels of urinary 8-isoprostane were elevated in diabetic *Ins2*$^{+/C96Y}$ mice compared with nondiabetic littermate control mice and further enhanced in diabetic *Ins2*$^{+/C96Y}$*Dusp4*$^{-/-}$ compared with diabetic *Ins2*$^{+/C96Y}$ mice (Fig. 8*F*). Expression of NOX4, one of the main sources of oxidant production in the kidney (38) and linked to podocyte dysfunction in diabetes (39,40), was increased by 30% in diabetic *Ins2*$^{+/C96Y}$ mice compared with nondiabetic *Ins2*$^{+/+}$ mice and exacerbated by 31% in diabetic *Ins2*$^{+/C96Y}$*Dusp4*$^{-/-}$ compared with diabetic *Ins2*$^{+/C96Y}$ mice (Fig. 8*G*).

DISCUSSION

Podocyte loss is one of the strongest markers of DN progression and is believed to be a driving factor in the development of the disease (4). Activation of MAPK by HG

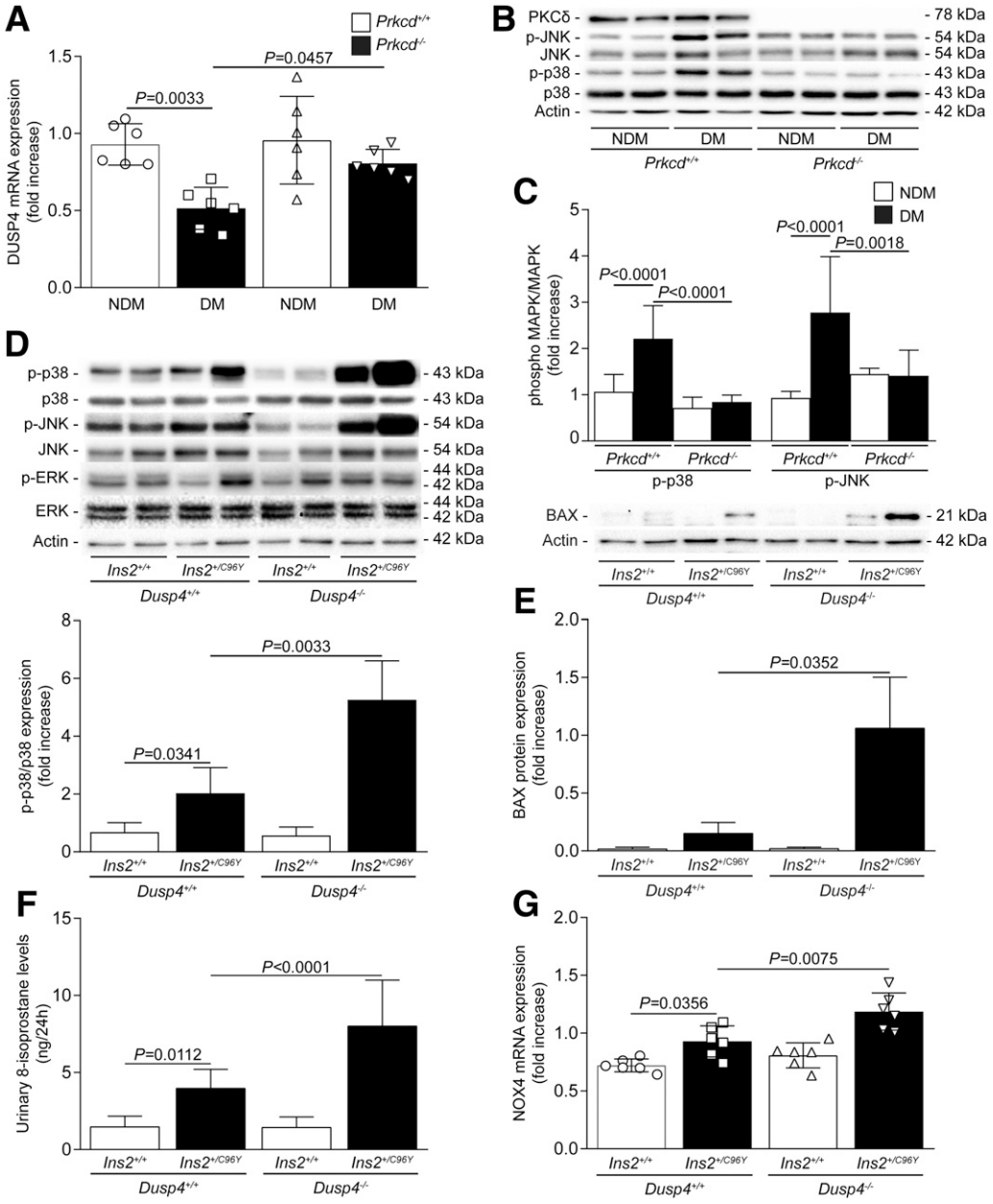

Figure 8— Loss of DUSP4 exacerbates p38 and JNK activation, systemic oxidant stress, and BAX and NOX4 expression in the renal cortex of *Ins2*$^{+/C96Y}$. Expression of DUSP4 mRNA (*A*) and p-p38, p38, p-JNK, JNK, and actin (*B*) from the renal cortex of nondiabetic (NDM) and diabetic (DM) *Prkcd*$^{+/+}$ and *Prkcd*$^{-/-}$ mice was detected by immunoblot, and densitometry quantitation (*C*) was measured. Expression of p38, JNK, and ERK phosphorylation (*D*), BAX (*E*), urinary 8-isoprostane levels (*F*), and NOX4 mRNA (*G*) from the renal cortex of 7-month-old *Ins2*$^{+/+}$, *Ins2*$^{+/C96Y}$, *Ins2*$^{+/+}$*Dusp4*$^{-/-}$, and Ins2$^{+/C96Y}$*Dusp4*$^{-/-}$ mice was measured by immunoblot (*D* and *E*), ELISA (*F*), and quantitative PCR (*G*). Results are shown as mean ± SD of 6 (*A* and *G*), 8 (*C*–*E*), and 10 (*F*) mice per group.

levels has been reported in multiple cell types and is linked to cellular disorder and development of microvascular pathologies (9). In podocytes, HF-induced activation of p38α MAPK enhanced DNA fragmentation, which can be prevented by the p38 inhibitor SB203580 (6). Although ample evidence shows that hyperglycemia activates MAPK in podocytes, the exact mechanisms leading to their activation have not been fully elucidated. In this study, we show for the first time that expression of DUSP4, a protein known to inhibit MAPK, was reduced by hyperglycemia in cultured podocytes and glomeruli. In addition, using *Dusp4*-deficient mice, we showed that loss of DUSP4 under hyperglycemic conditions is associated with sustained activation of both p38 and JNK, enhanced albuminuria, glomerular fibrosis, podocyte dysfunction, and foot process effacement. More interestingly, reduced DUSP4 expression, and not DUSP1, in the renal cortex of patients with diabetes correlated with lower eGFR levels.

Chronic activation of the p38 MAPK pathway was originally discovered to promote cell death caused by cellular stresses. It is often associated with diverse disease pathology, including inflammation, ischemia/reperfusion injury, infectious disease, and neuronal disease (41). In the glomeruli of diabetic animals, p38 MAPK activity was enhanced compared with their nondiabetic counterparts (7,42). Inhibition of p38 activity was associated with decreased expression of extracellular matrix proteins, Col IV, fibronectin, and TGF-β (15). Our results corroborate these observations. The absence of DUSP4 enhanced the activation of both p38 and JNK in $Ins2^{+/C96Y}Dusp4^{-/-}$ mice and was associated with increased glomerular fibrosis and fibrotic gene expression.

Activation of p38 and JNK is associated with increased podocyte cell death through upregulation of BAX (29,40). Our current results support the notion that sustained activation of p38 and JNK MAPK in diabetic DUSP4-deficient mice markedly enhanced BAX expression. Moreover, overexpression of DUSP4 in podocytes prevented the HG-induced activation of p38 and JNK, which normalized both caspase 3/7 enzymatic activity and BAX expression to NG levels. These results further support the idea that activation of p38 and JNK MAPK in DN promotes loss of podocytes through increased cell death signals.

The mechanisms by which diabetes regulates DUSP expression and activity in the kidney have never been explored. Previous studies showed that activation of PKC-δ decreased DUSP1 expression (31,32). Interestingly, activation of PKC-δ by hyperglycemia has been linked to sustained activation of p38 in retinal pericytes and podocytes (6,9). Our data uncovered another pathway of PKC-δ–induced p38 MAPK activation through DUSP deregulation. Inhibition of PKC-δ expression in diabetic mice and podocytes exposed to HG concentrations prevented DUSP4 reduction and phosphorylation of p38 and JNK MAPK without affecting other DUSP expression. These results combined with other studies suggest that diabetes and hyperglycemia cause podocyte dysfunction mainly through the activation of PKC-δ and p38 MAPK, in part, mediated by reduced DUSP4 expression.

For many years, an excess in cellular glucose substrate availability was postulated to generate reactive oxygen species (ROS), which in turn drives vascular complications in DN (43). However, this hypothesis has been challenged by the negative results of antioxidant-based clinical trials (44). ROS production in DN has been linked to podocyte dysfunction, and mice with podocyte-specific genetic deletion of NOX4, the main source of ROS in the kidney, are protected from developing glomerular damage (39,45). Moreover, downregulation of DUSP4 expression in $Dusp4^{-/-}$ with siRNA in cardiomyocytes resulted in increased NOX4 expression (46), whereas overexpression of DUSP4 in endothelial cells reduced hypoxia/reoxygenation-induced oxidative stress (47). Our results indicate that loss of DUSP4 expression caused by HG levels could contribute to oxidant production, because deletion of DUSP4 enhanced NOX4 expression in diabetic mice while overexpression of DUSP4 in podocytes prevented NOX4 and HO-1 expression.

Studies trying to evaluate DUSP4 specificity toward MAPK showed that it can be influenced both by cell type and mechanism, leading to MAPK activation. In most cancer cell lineages, DUSP4 activity is linked to reduced ERK phosphorylation in the nucleus (48). In macrophages, overexpression of DUSP4 prevented tumor necrosis factor-α–induced activation of both p38 and JNK MAPK (49), whereas knockdown of DUSP4 in MH-S cells led to increased ERK phosphorylation after lipopolysaccharide was administered (50). In cardiomyocytes, genetic deletion of both DUSP1 and DUSP4 resulted in sustained activation of p38 MAPK, while the phosphorylation levels of JNK and ERK remained unchanged (23). Our data showed that in the glomeruli and in podocytes under HG conditions, DUSP4 activity seems specific to both p38 MAPK and JNK, while phosphorylation levels of ERK were unaffected by modulation of DUSP4 expression. The expression levels of other DUSPs might partly explain the different profile of MAPK phosphorylation status observed in different cell types. In addition, our data demonstrated that DUSP4 mRNA expression was decreased in the tubular cell fraction. We therefore cannot exclude the potential impact of DUSP4 reduction in tubules to DN progression. However, Akita mice do not produce severe tubular fibrosis. Thus, additional experiments using a more appropriate mouse model of tubular fibrosis will be required in future studies to evaluate the impact of reduced DUSP4 expression in the tubules.

In conclusion, our study showed that hyperglycemia reduces DUSP4 expression in cultured podocytes and renal tissue of diabetic mice and patients with diabetes. Loss of DUSP4 expression in a context of diabetes contributed to sustained activation of p38 and JNK MAPK, oxidant production, and cell death that resulted in glomerular injury and dysfunction and effacement of podocytes. These results strongly suggest that preventing loss of DUSP4

expression in DN could present an interesting avenue to stop podocyte loss and halt the progression of DN.

Acknowledgments. The authors gratefully acknowledge Anne Vezina (Histology Core, University of Sherbrooke) for her assistance.

Funding. This work was supported by grants from the Canadian Institutes of Health Research, Institute of Nutrition, Metabolism and Diabetes (PJT153165 and 201505MOP to P.G.). This work was performed at the CHU de Sherbrooke Research Center, funded by the "Fonds de Recherche du Québec–Santé." P.G. is currently the holder of the Canada Research Chair in Vascular Complications of Diabetes.

Duality of Interest. No potential conflicts of interest relevant to this article were reported.

Author Contributions. B.D., M.R., D.-A.D., and F.L. performed experiments and researched data. B.D., F.L., A.M.C., and P.G. analyzed the data and wrote the manuscript. A.G. performed animal care. M.A.-M. provided the DUSP4 adenovirus and *Dusp4*$^{-/-}$ mice. P.G. is the guarantor of this work, had full access to all the data, and, as such, had full access to all the data in the study and takes responsibility for the integrity of the data and the accuracy of the data analysis.

References

1. Collins AJ, Kasiske B, Herzog C, et al. Excerpts from the United States Renal Data System 2006 Annual Data Report. Am J Kidney Dis 2007;49(Suppl. 1):A6–A7, S1–S296
2. Greka A, Mundel P. Cell biology and pathology of podocytes. Annu Rev Physiol 2012;74:299–323
3. Powell DW, Kenagy DN, Zheng S, et al. Associations between structural and functional changes to the kidney in diabetic humans and mice. Life Sci 2013;93:257–264
4. Meyer TW, Bennett PH, Nelson RG. Podocyte number predicts long-term urinary albumin excretion in Pima Indians with Type II diabetes and microalbuminuria. Diabetologia 1999;42:1341–1344
5. Lizotte F, Denhez B, Guay A, Gévry N, Côté AM, Geraldes P. Persistent insulin resistance in podocytes caused by epigenetic changes of SHP-1 in diabetes. Diabetes 2016;65:3705–3717
6. Mima A, Kitada M, Geraldes P, et al. Glomerular VEGF resistance induced by PKCδ/SHP-1 activation and contribution to diabetic nephropathy. FASEB J 2012;26:2963–2974
7. Igarashi M, Wakasaki H, Takahara N, et al. Glucose or diabetes activates p38 mitogen-activated protein kinase via different pathways. J Clin Invest 1999;103:185–195
8. Hirosumi J, Tuncman G, Chang L, et al. A central role for JNK in obesity and insulin resistance. Nature 2002;420:333–336
9. Geraldes P, Hiraoka-Yamamoto J, Matsumoto M, et al. Activation of PKC-delta and SHP-1 by hyperglycemia causes vascular cell apoptosis and diabetic retinopathy. Nat Med 2009;15:1298–1306
10. Nakagami H, Morishita R, Yamamoto K, et al. Phosphorylation of p38 mitogen-activated protein kinase downstream of bax-caspase-3 pathway leads to cell death induced by high D-glucose in human endothelial cells. Diabetes 2001;50:1472–1481
11. Sakai N, Wada T, Furuichi K, et al. Involvement of extracellular signal-regulated kinase and p38 in human diabetic nephropathy. Am J Kidney Dis 2005;45:54–65
12. Adhikary L, Chow F, Nikolic-Paterson DJ, et al. Abnormal p38 mitogen-activated protein kinase signalling in human and experimental diabetic nephropathy. Diabetologia 2004;47:1210–1222
13. Kang SW, Adler SG, Lapage J, Natarajan R. p38 MAPK and MAPK kinase 3/6 mRNA and activities are increased in early diabetic glomeruli. Kidney Int 2001;60:543–552
14. Jung DS, Li JJ, Kwak SJ, et al. FR167653 inhibits fibronectin expression and apoptosis in diabetic glomeruli and in high-glucose-stimulated mesangial cells. Am J Physiol Renal Physiol 2008;295:F595–F604
15. Tesch GH, Ma FY, Han Y, Liles JT, Breckenridge DG, Nikolic-Paterson DJ. ASK1 inhibitor halts progression of diabetic nephropathy in Nos3-deficient mice. Diabetes 2015;64:3903–3913
16. Doggrell SA, Christensen AM. Does the p38 MAP kinase inhibitor pamapimod have potential for the treatment of rheumatoid arthritis? Expert Opin Pharmacother 2010;11:2437–2442
17. Dickinson RJ, Keyse SM. Diverse physiological functions for dual-specificity MAP kinase phosphatases. J Cell Sci 2006;119:4607–4615
18. Kondoh K, Nishida E. Regulation of MAP kinases by MAP kinase phosphatases. Biochim Biophys Acta 2007;1773:1227–1237
19. Xu H, Dembski M, Yang Q, et al. Dual specificity mitogen-activated protein (MAP) kinase phosphatase-4 plays a potential role in insulin resistance. J Biol Chem 2003;278:30187–30192
20. Emanuelli B, Eberlé D, Suzuki R, Kahn CR. Overexpression of the dual-specificity phosphatase MKP-4/DUSP-9 protects against stress-induced insulin resistance. Proc Natl Acad Sci U S A 2008;105:3545–3550
21. Wu JJ, Roth RJ, Anderson EJ, et al. Mice lacking MAP kinase phosphatase-1 have enhanced MAP kinase activity and resistance to diet-induced obesity. Cell Metab 2006;4:61–73
22. Wu Z, Jiao P, Huang X, et al. MAPK phosphatase-3 promotes hepatic gluconeogenesis through dephosphorylation of forkhead box O1 in mice. J Clin Invest 2010;120:3901–3911
23. Auger-Messier M, Accornero F, Goonasekera SA, et al. Unrestrained p38 MAPK activation in Dusp1/4 double-null mice induces cardiomyopathy. Circ Res 2013;112:48–56
24. Keyse SM. Protein phosphatases and the regulation of mitogen-activated protein kinase signalling. Curr Opin Cell Biol 2000;12:186–192
25. Lizotte F, Paré M, Denhez B, Leitges M, Guay A, Geraldes P. PKCδ impaired vessel formation and angiogenic factor expression in diabetic ischemic limbs. Diabetes 2013;62:2948–2957
26. Drapeau N, Lizotte F, Denhez B, Guay A, Kennedy CR, Geraldes P. Expression of SHP-1 induced by hyperglycemia prevents insulin actions in podocytes. Am J Physiol Endocrinol Metab 2013;304:E1188–E1198
27. Keir LS, Firth R, May C, Ni L, Welsh GI, Saleem MA. Generating conditionally immortalised podocyte cell lines from wild-type mice. Nephron 2015;129:128–136
28. Levey AS, Stevens LA, Schmid CH, et al.; CKD-EPI (Chronic Kidney Disease Epidemiology Collaboration). A new equation to estimate glomerular filtration rate. Ann Intern Med 2009;150:604–612
29. Liu WT, Peng FF, Li HY, et al. Metadherin facilitates podocyte apoptosis in diabetic nephropathy. Cell Death Dis 2016;7:e2477
30. Li R, Zhang L, Shi W, et al. NFAT2 mediates high glucose-induced glomerular podocyte apoptosis through increased Bax expression. Exp Cell Res 2013;319:992–1000
31. Choi BH, Hur EM, Lee JH, Jun DJ, Kim KT. Protein kinase Cdelta-mediated proteasomal degradation of MAP kinase phosphatase-1 contributes to glutamate-induced neuronal cell death. J Cell Sci 2006;119:1329–1340
32. Lomonaco SL, Kahana S, Blass M, et al. Phosphorylation of protein kinase Cdelta on distinct tyrosine residues induces sustained activation of Erk1/2 via down-regulation of MKP-1: role in the apoptotic effect of etoposide. J Biol Chem 2008;283:17731–17739
33. Sharma K, Ramachandrarao S, Qiu G, et al. Adiponectin regulates albuminuria and podocyte function in mice. J Clin Invest 2008;118:1645–1656
34. Koshikawa M, Mukoyama M, Mori K, et al. Role of p38 mitogen-activated protein kinase activation in podocyte injury and proteinuria in experimental nephrotic syndrome. J Am Soc Nephrol 2005;16:2690–2701
35. Lim AK, Ma FY, Nikolic-Paterson DJ, et al. Evaluation of JNK blockade as an early intervention treatment for type 1 diabetic nephropathy in hypertensive rats. Am J Nephrol 2011;34:337–346
36. Ijaz A, Tejada T, Catanuto P, et al. Inhibition of C-jun N-terminal kinase improves insulin sensitivity but worsens albuminuria in experimental diabetes. Kidney Int 2009;75:381–388

37. Azushima K, Gurley SB, Coffman TM. Modelling diabetic nephropathy in mice. Nat Rev Nephrol 2018;14:48–56
38. Sedeek M, Nasrallah R, Touyz RM, Hébert RL. NADPH oxidases, reactive oxygen species, and the kidney: friend and foe. J Am Soc Nephrol 2013;24:1512–1518
39. Jha JC, Thallas-Bonke V, Banal C, et al. Podocyte-specific Nox4 deletion affords renoprotection in a mouse model of diabetic nephropathy. Diabetologia 2016;59:379–389
40. Jha JC, Gray SP, Barit D, et al. Genetic targeting or pharmacologic inhibition of NADPH oxidase nox4 provides renoprotection in long-term diabetic nephropathy. J Am Soc Nephrol 2014;25:1237–1254
41. Obata T, Brown GE, Yaffe MB. MAP kinase pathways activated by stress: the p38 MAPK pathway. Crit Care Med 2000;28(Suppl.):N67–N77
42. Dunlop ME, Muggli EE. Small heat shock protein alteration provides a mechanism to reduce mesangial cell contractility in diabetes and oxidative stress. Kidney Int 2000;57:464–475
43. Brownlee M. Biochemistry and molecular cell biology of diabetic complications. Nature 2001;414:813–820
44. de Zeeuw D, Akizawa T, Audhya P, et al.; BEACON Trial Investigators. Bardoxolone methyl in type 2 diabetes and stage 4 chronic kidney disease. N Engl J Med 2013;369:2492–2503
45. Susztak K, Raff AC, Schiffer M, Böttinger EP. Glucose-induced reactive oxygen species cause apoptosis of podocytes and podocyte depletion at the onset of diabetic nephropathy. Diabetes 2006;55:225–233
46. Barajas-Espinosa A, Basye A, Angelos MG, Chen CA. Modulation of p38 kinase by DUSP4 is important in regulating cardiovascular function under oxidative stress. Free Radic Biol Med 2015;89:170–181
47. Dougherty JA, Kilbane Myers J, Khan M, Angelos MG, Chen CA. Dual-specificity phosphatase 4 overexpression in cells prevents hypoxia/reoxygenation-induced apoptosis *via* the upregulation of eNOS. Front Cardiovasc Med 2017;4:22
48. Balko JM, Cook RS, Vaught DB, et al. Profiling of residual breast cancers after neoadjuvant chemotherapy identifies DUSP4 deficiency as a mechanism of drug resistance. Nat Med 2012;18:1052–1059
49. Jiao H, Tang P, Zhang Y. MAP kinase phosphatase 2 regulates macrophage-adipocyte interaction. PLoS One 2015;10:e0120755
50. Cornell TT, Fleszar A, McHugh W, Blatt NB, Le Vine AM, Shanley TP. Mitogen-activated protein kinase phosphatase 2, MKP-2, regulates early inflammation in acute lung injury. Am J Physiol Lung Cell Mol Physiol 2012; 303:L251–L258